

Practical, Stretchable Smart Skin Sensors for Contact-Aware Robots in Safe and Collaborative Interactions

John O'Neill, Jason Lu, Rodney Dockett and Timothy Kowalewski Ph.D.

Abstract—Safe, intuitive human-robot interaction requires that robots intelligently interface with their environments, ideally sensing and localizing physical contact across their link surfaces. We introduce a stretchable smart skin sensor that provides this function. Stretchability allows it to conform to arbitrary robotic link surfaces. It senses contact over nearly the entire surface, localizes contact position of a typical finger touch continuously over its entire surface ($RMSE = 7.02mm$ for a $14.7cm \times 14.7cm$ area), and provides an estimate of the contact force. Our approach exclusively employs stretchable, flexible materials resulting in skin strains of up to 150%. We exploit novel carbon nanotube elastomers to create a two-dimensional potentiometer surface. Finite element simulations validate a simplified polynomial surface model to enable real-time processing on a basic microcontroller with no supporting electronics. Using only five electrodes, the skin can be scaled up to arbitrary sizes without needing additional electrodes. We designed, implemented, calibrated, and tested a prototype smart skin as a tactile sensor on a custom medical robot for sensing unexpected physical interactions. We experimentally demonstrate its utility in collaborative robotic applications by showing its potential to enable safer, more intuitive human-robot interaction.

I. INTRODUCTION

Robotic systems in industrial, home, and medical applications have increasingly required the ability to work safely in collaborative environments with humans. In order to safely work around humans, multiple sensing modalities and joint configurations have been utilized with varying levels of success [1]. The primary need in this field is an affordable, modular sensing system—such as a skin with minimal wiring—that could be applied to any robotic link regardless of geometry and material. Ideally, like human skin, this system should detect physical contact, localize its position on the link, and assess the magnitude of the force [2]. By covering each link of a robotic arm with a tactile sensing skin, robots could gain increased awareness of their physical interactions with unpredictable environments or human activity. This would enable humans and robots to collaborate more safely and intuitively in a variety of situations. For example, in robotic surgery human arms and robotic manipulators must compete for access to a highly constrained workspace. A surgeon and scrub nurse can achieve this by letting their arms collide and remain in contact. Unlike with a traditional robot, the surgeon can intuitively push and the nurse will temporarily move away to allow access without the need for verbal communication.

Department of Mechanical Engineering, University of Minnesota, Minneapolis, MN, 55414, USA oneil1463@umn.edu

Several industrial robots have utilized ‘soft’ joint configurations to avoid harmful collisions. The Baxter Robot (ReThink Robotics, Boston, MA) employs motor-driven spring joints which require complex and specialized designs. These specialized joints also complicate controls algorithms. Other methods have included computer vision algorithms for collision avoidance, however computer vision algorithms typically suffer from line-of-sight and accuracy limitations.

Prior art has also considered smart skins: flexible materials embedded with force or position sensors which can be molded to different geometries. Several attempts at smart skins have utilized arrays of rigid force sensors embedded in flexible media such as a flexible printed circuit board or polydimethylsiloxane (PDMS) silicone. Force sensors include standard strain gauges [3], piezoresistive sensors [4], capacitive force sensors [5], and polyvinylidene fluoride (PVDF) sensors [6]. The issue with the use of rigid sensors in flexible media is that the device is still not stretchable. A second issue with sensor arrays is that contact position and force data are limited to tactile pixels (taxels): finite locations separated by deadzones. Even as sensors get smaller, sensing is limited to discrete positions in the 2D plane. Moreover there is a linear increase in the number of electrodes ($2n$) for increases in sensing area ($n \times n$), even if multiplexed.

Given the shortcomings in rigid sensor arrays, research groups have instead focused on developing flexible sensor pads for smart skin sensing applications. Choi et al. designed a tactile sensor based on $0.5mm^2$ PVDF sensor arrays embedded in polyester film [7]. While these small PVDF sensors allow more flexibility than the larger sensor arrays, they still suffer from large numbers of electrodes. Papakostas et al. also developed a flexible tactile sensor comprised of polyester sheets embedded with a grid of silver-polymer conductive traces [8]. The grid contacts form a piezoresistive force sensor. The grid of conductive traces allows for flexibility in both the sensors and medium. However, this solution still requires n^2 electrodes for an $n \times n$ sensor array. In order to cover the smoothly curving, swept geometry of robotic arms such as the Kuka LBR (KUKA Roboter GmbH, Augsburg Germany) or the Baxter, a smart skin needs to be both flexible and *stretchable*. A stretchable two-dimensional skin that conforms to arbitrary geometries is also easier to manufacture than 3-dimensional skins specifically made to fit a particular robot geometry.

Pugach et al. have proposed a method involving conductive rubber sheets created by mixing carbon into the material [9]. Using electrical impedance tomography, a series of many electrodes situated around the perimeter of the conductive

surface are used to sense and localize tactile force. While this group was able to achieve successful calibration and sensing using this method, this design suffers drawbacks such as the requirement that forces be applied by conductive materials which is not the case in collaborative environments. This approach does not scale well with large areas while maintaining spatial and temporal resolution. The electrodes situated around the perimeter require the number of interconnected wires to scale by $4n$ for n^2 discrete taxels. Additionally it is unclear whether this design can endure the necessary stretching for conforming to varied robotic link geometry.

Lacasse et al. demonstrated a flexible skin sensor based on carbon black (CB)-filled silicone and conductive fabric [10]. The CB silicone and conductive fabric is then cut into individual strips and woven to form a sensing grid of discrete taxels. The resistance in each discrete sensor in the grid is then independently measured using an inverting amplifier. A considerable merit of this approach is that it is stretchable. However, the use of discrete sensors remains a drawback in terms of discrete position sensing and potential for dead zones. The discrete sensors again require a large number of wire interconnects ($2n$ wires for n^2 discrete taxels). Additionally the use of silicone PDMS carbon black as a force sensor requires system identification and dynamic calibration due to the visco-elastic properties of silicone that confound force measurement with time. This negatively impacts the variety of geometry available, ease of manufacturing, and complexity of electronics and processing required.

To date, there exists no inexpensive, stretchable skin sensor that is simultaneously 1) scalable (e.g. constant electrode count for increased surface area without decrease in temporal resolution or relative spatial position resolution); 2) provides continuous force and position sensing (without dead zones or limited taxels); 3) can be easily manufactured; 4) requires minimal electronics and processing, and 5) can be easily adapted to fit modern robot link surfaces. We herein propose such a solution. We exploit a novel carbon nanotube (CNT)-doped PDMS elastomer sheet to meet these needs by implementing a 2D potentiometer similar to the work initially proposed by Walz et al. as a low-cost tool-tissue tracking method for surgical simulation [11]. We document the design, practical implementation, and accuracy of this system and demonstrate its utility in collaborative robotic applications.

II. METHODS

A. Sensor Design

The proposed smart skin sensor consists of three layers of flexible, stretchable materials (Fig. 1). The top layer (Ag-nylon) is silver-coated conductive fabric (Medtex, Staxtex Productions, Bremen, Germany). The middle layer is non-conductive perforated cloth (Powermesh Fabric, 99% polyester, 1% spandex). The bottom layer (See Fig. 2b for detail) consists of a 1.75mm PDMS substrate with a uniform, bonded $100\mu\text{m}$ CNT-PDMS coating (7-SIGMA Inc., Minneapolis MN). The layers are cut into the desired

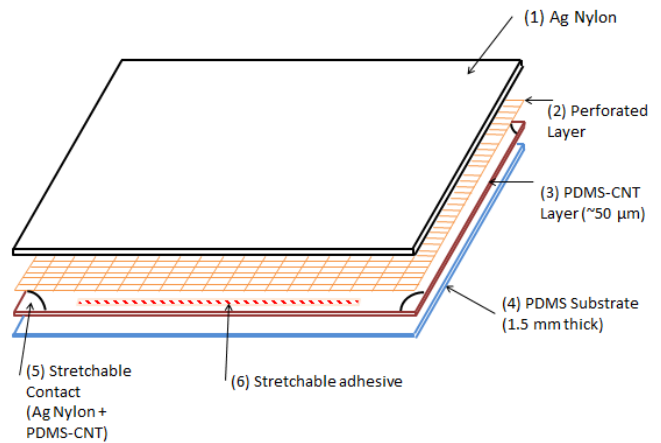


Fig. 1. Side view of CNT skin sensor.

pad dimensions ($14.7 \times 14.7\text{cm}$, Fig. 2a) then bonded via non-conductive PDMS adhesive (7-SIGMA).

The electrodes are cut into 1cm -radius quarter circles from silver conductive cloth infused with the CNT-PDMS resin material and heat cured onto bottom layer (Fig. 2). A single wire is then conductively bonded to each cloth electrode. A contact resistance of about 500Ω is achieved while maintaining a stretchable and flexible mechanical properties at the electrode locations. In this embodiment, the bottom layer exhibits an overall resistance of approximately $1.85\text{k}\Omega$ between corner electrodes.

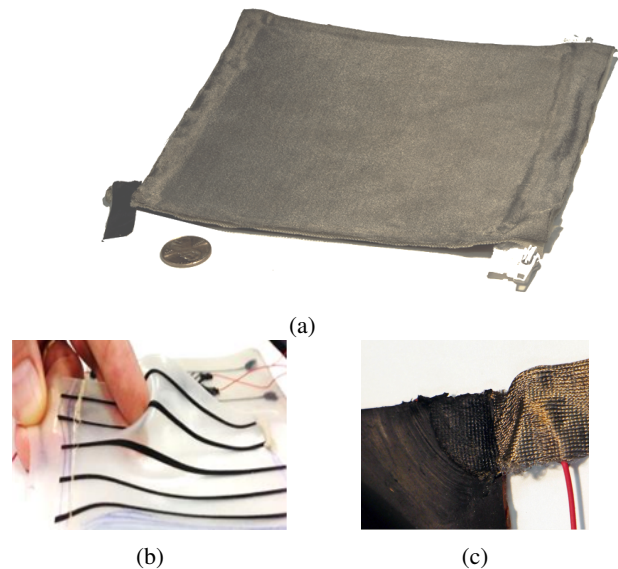


Fig. 2. (a) the assembled smart skin with bonded zippers for easier attachment, (b) a close-up of the PDMS substrate with CNT stripes to indicate stretch, and (c) close-up of CNT PDMS conductive cloth contact detail.

To quantitatively analyze human interaction a synthetic replica of an adult male index finger was created by casting A35 durometer silicone rubber (PlatSil 71-35 Polytek Development, Easton, PA) to emulate typical human tactile

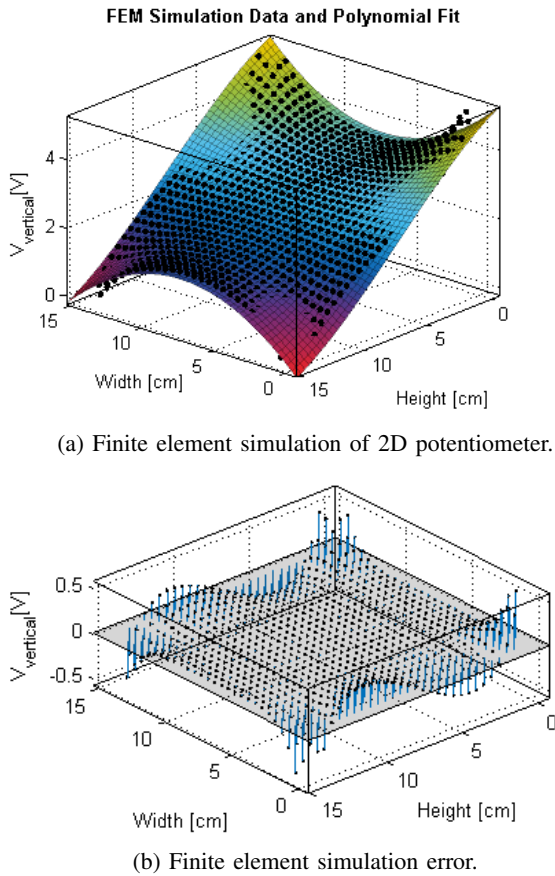


Fig. 3. Finite Element Simulation

interaction. A 6.5mm diameter wooden dowel was inserted in the finger for internal skeletal structure and repeatable attachment to load cells.

B. 2D Potentiometer FEM Simulation and Model

We modified the approach of [11] to create a finite element model of the voltage as a function of two-dimensional position with a rectangular 14.7cm × 14.7cm Neumann boundary and quarter-circle pads (1cm radius) as Dirichlet boundaries. MATLAB's (MathWorks Natick, MA) Partial Differential Equation toolbox numerically solved the DC conduction diffusion problem: $-\nabla \cdot (\sigma \nabla(V)) = q, E = \nabla(V)$, with $V = 5\text{volts}$ and a mesh of $n = 2701$ nodes. The simulation results are shown in Fig. 3a for a single permutation of corner electrode voltages.

To enable real-time processing on a microcontroller we employed a simplified polynomial surface model using least squares regression with bisquare robustness correction to fit coefficients. Given the odd and even symmetry displayed in Fig. 3a we chose cubic and quadratic terms. Fig. 3b shows the fit with $R^2 = 0.995$ and that the error is confined to the corners and boundaries. Given this strong fit and lowest-possible model complexity (polynomial order) for the observed curvature, we assumed there was no overfitting and adopted this polynomial model to represent the complexity of our mapping between two-dimensional measured voltages

and positions.

C. Electronics and Algorithm Design

In order to achieve a high degree of accuracy using the least amount of wires, four conductive nodes were attached to the smart skin, one at each corner. The four corner electrodes (nodes) and top fabric layer were wired directly to programmable GPIO pins of a simple microcontroller (ATmega328, Atmel Corporation, San Jose CA). The microcontroller allows changing each node to either V_{dd} , ground, high impedance or analog input. For position measurements, the microcontroller was programmed such that the top fabric layer acts as a high impedance analog-to-digital converter and the CNT skin is rapidly pulsed in alternating configurations. Two adjacent terminals were set to V_{dd} , while the other two were set to ground. The conductive fabric voltage was measured, then the voltage values were rotated clockwise and the voltage measured again. The final two iterations are simply the opposite of the first two, providing another data point to average with the first. These two primary direction voltages are seen as the first two rows in TABLE I and the node/pin assignments in Fig. 4.

For force estimation, the top fabric was set to either V_{dd} or ground. One of the nodes was used as an analog to digital converter in order to measure the ratio of contact resistance to the bulk resistance of the pad. The contact resistance is proportional to the contact force: higher forces result in lower contact resistance for a constant contact area but more finger force also allows more perforated holes to make contact, increasing the effective contact area. The setup can be rotated in a similar manner to the directional setup, and additionally the node configuration can be flipped. The fabric can be either V_{dd} or ground, yielding a total of 16 permutations (of which eight are merely opposites). The highest value of the eight is used, in order to utilize the maximum dynamic range across the pad.

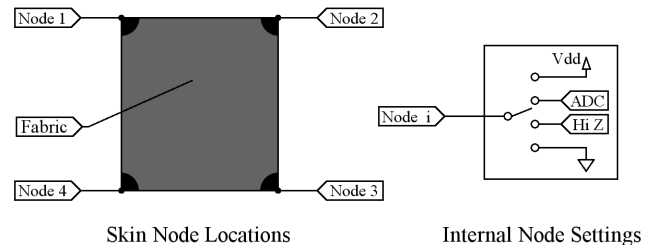


Fig. 4. Smart skin schematic.

Since the force estimation and position estimation algorithms require different node setups, each estimation cannot be taken simultaneously. However by electronically switching the electrode values, position and force can be read in an alternating fashion. The switching and reading for each mode requires approximately 1ms. This allows complete force and position information readings of 2ms.

The system was assumed third-order, since it was adequately described by a two by three polynomial surface with

voltage as a function of positions in section II-B. The inverse mapping, with position as a function of voltages is thus expected to also follow a third order polynomial, and the equation for the position is a two by three polynomial surface with cross terms, where the third order term goes along the direction in question (Eq. 1). For example, to calculate X, the V_{horiz} that increases is used as the third-order term:

$$X = \begin{bmatrix} V_h^3 & V_h^2 V_v & V_h V_v^2 & V_h^2 & V_v^2 & V_h & V_v & 1 \\ a_7 & a_6 & a_5 & a_4 & a_3 & a_2 & a_1 & a_0 \end{bmatrix}^T \quad (1)$$

This equation was fitted to the calibration data, then implemented in the microcontroller to provide real-time position data to the robot controller for the collaborative interaction experiment.

The equation for the force is a cubic model from the maximum of the eight permutations of node voltage (Eq. 2). This automatically ignores sensor values from quadrants not near the location of force application. The equation was fitted to the calibration data, then implemented in the microcontroller.

$$f = b_0 + b_1 \max(V_{f1} : V_{f8}) \quad (2)$$

Force values above a threshold assume a touch had occurred. This information is then either sent to a relay on the robot's emergency stop circuit for the emergency stop experiment, or used to verify the validity of touch for the collaborative interaction experiment.

D. Calibration For Typical Human Tactile Interaction

The smart skin design requires calibration in terms of both position of force application as well as force magnitude. In order to calibrate the 2D position sensing, a routine was established wherein a fixed force was applied to the skin in known locations along a regular 2D grid. The known x-y locations and the measured voltage potentials were recorded for each point on the grid. This data was then applied to a BiSquare least squares fit in MATLAB in order to fit to the 3rd order polynomial described in Section II-C.

Node #	1	2	3	4	Fabric
V_{vert}	Gnd	Gnd	V_{dd}	V_{dd}	ADC
V_{horiz}	Gnd	V_{dd}	V_{dd}	Gnd	ADC
\vdots	\vdots	\vdots	\vdots	\vdots	ADC

TABLE I. Permutations used for position.

Node #	1	2	3	4	Fabric
V_{f1}	Gnd	Gnd	ADC	HiZ	V_{dd}
V_{f1}	Gnd	Gnd	HiZ	ADC	V_{dd}
V_{f1}	Gnd	HiZ	ADC	Gnd	V_{dd}
\vdots	\vdots	\vdots	\vdots	\vdots	\vdots
V_{f8}	HiZ	ADC	V_{dd}	V_{dd}	Gnd

TABLE II. Permutations used for force.

In order to apply a known force in a known x-y grid, a custom robotic arm, CORVUS, was used [12]. The CORVUS arm was outfitted with an end effector comprised of the conformable replicate finger mold (Fig. 5) described in section II-A. The force was controlled by maintaining a constant compression of the replicate finger through position control. Force was also monitored through a load cell to ensure a stable force was being applied. The x-y grid used a 1cm separation in each dimension on a sample skin area of 144cm².

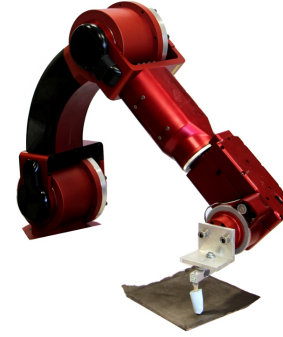


Fig. 5. A custom robotic arm was used to calibrate position sensing in typical human tactile interactions by applying known forces in a known 2D grid via a human finger replica.

To calibrate force, the load cell on the synthetic finger was used to measure the interaction force, while all of the voltage permutations were measured. Both sensors recorded at 30Hz throughout the touch. This test was performed at the center of the pad.

The load cell data was synchronously recorded along with the voltage values. This data was then fit to the proposed polynomial surface model where the dependent variable is the maximum of the eight node voltage permutations as described in section II-C. The results of this fit can be found in section III.

E. Experimental Design

To evaluate the functional response of the smart skin, the skin was mounted to conform to the surface of a distal link of the CORVUS robot (Fig.6). The skin was connected to the emergency stop circuit by means of a solid state relay. The skin's microcontroller was programmed to sample at 150Hz and respond to any touch with non-zero force by enabling the robot's emergency stop circuit. The robot was then commanded a trajectory which ran at 3mm/s and intercepted the synthetic finger attached to a load cell (Fig.6). During the experiment, emergency stop state and force data was collected. This experiment was repeated 20 times to test repeatability.

In order to functionally verify the skin's positional response in human-robot interactions, the skin was placed on the CORVUS robot as above but a human operator pushed on the link with an index finger. Then, the microcontroller was set to determine if a valid touch had occurred, and if so, output the position of a touch. The robot was programmed

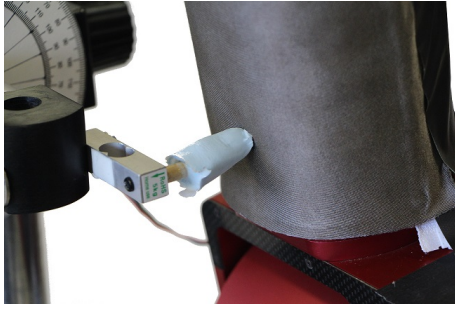


Fig. 6. Known forces were applied to the skin mounted on a link via the silicone cast finger attached to a load cell.

to respond to touches by moving in the opposite direction. The location of contact provided by the skin determined this direction based on the geometry of the link. The direction was assumed to be normal to the skin, so the robot would move directly away from the finger. The synthetic finger attached to a load cell was moved toward the robot while maintaining a constant velocity, with the robot either set to take evasive action or remain still.

III. RESULTS

The construction of the smart skin resulted in a highly stretchable and flexible surface. The electrical properties of the skin such as conductivity did not change significantly with the repeated application of stress. As shown in figure 7b, the skin is capable of stretch to approximately 150% of the original size.

The skin was successfully applied to the irregular surface of the CORVUS robot arm, and functioned on the arm. The skin installed on the robot arm can be seen in Fig. 7a.

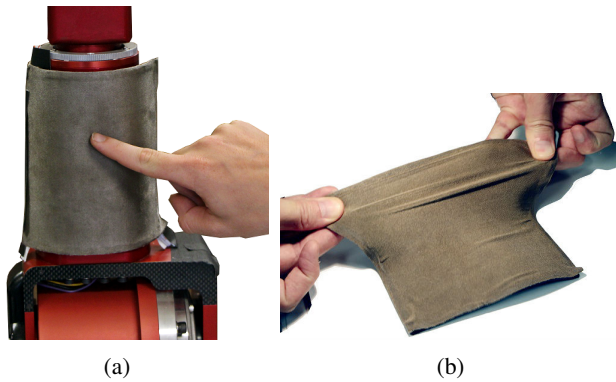


Fig. 7. Evidence of (a) successful conformation to a link surface and (b) of stretching near 150% (b).

Using the x-y calibration data of potential, force and location, the least squares fit was run to determine the coefficients for the polynomial. The coefficients were computed with R^2 values of 0.9934 for the X-Fit and 0.9978 for Y-Fit. The mean absolute error was 3.32mm and RMSE was 7.02mm. 90% of all error was below 5.7mm, and the highest error was at the corners and boundaries as predicted by Fig. 3a. The 3D plot of the polynomial in X Cartesian space plotted

alongside the calibration points is shown in Fig. 8, and the polynomial in Y Cartesian space is very similar.

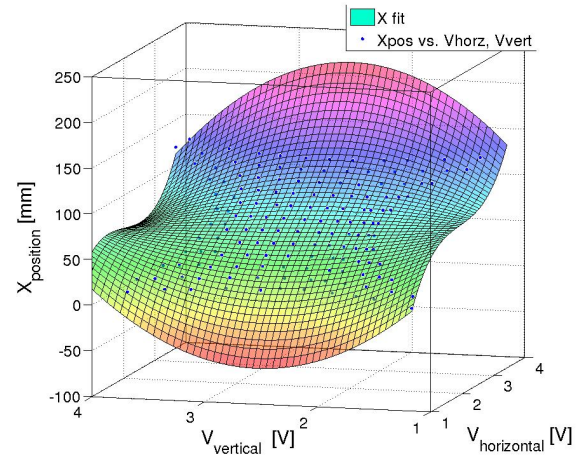


Fig. 8. Polynomial fit in X ($R^2 = 0.9934$).

The force measured by the load cell is plotted against the maximum of the node voltages for 144 separate touch incidents located at the center of the pad (Fig. 9). A cubic model relating load cell force and maximum node voltage was fitted with an R^2 value of 0.7270.

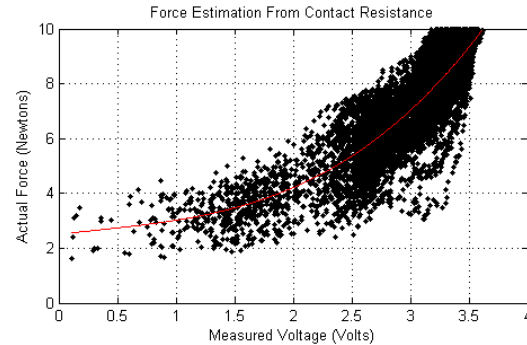


Fig. 9. Cubic fit of force to node voltage.

The smart skin's response to a finger touch is shown in Fig. 10. The vertical line shows the skin's triggering of an emergency stop event. The green horizontal line shows the force at which the skin triggers that a touch has occurred, which was at 0.5 N. Beyond the point where the emergency stop was triggered, the forces represent the dynamics of the robot, in this case the brakes take approximately 100ms to fully stop the robot, and oscillations continue beyond that point. The skin successfully detected the touch and brought the robot to a halt for all 20 iterations of the experiment.

The result of the collaborative control experiment is shown in Fig. 11. The control test without evasive action rapidly reaches the limit of the load cell and does not decrease, as the target position is never achieved. However, with evasive action triggered by the contact data from the smart skin sensor the force is maintained at approximately 11N, which is below an example critical force of 12.5N, until the target position is reached.

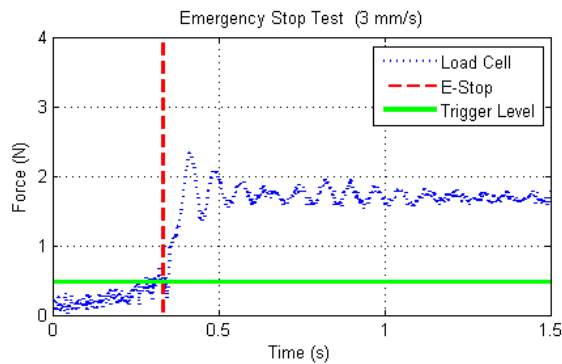


Fig. 10. Force on finger with emergency stop.

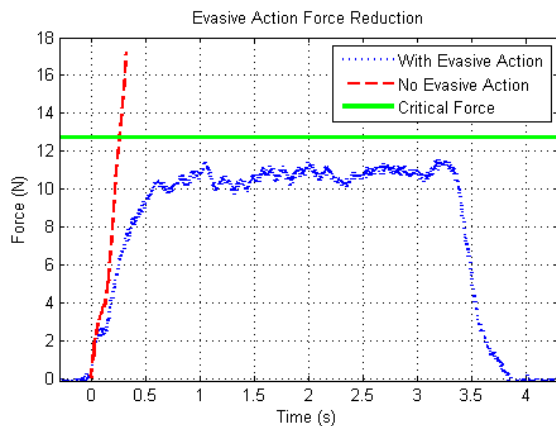


Fig. 11. Force on finger with evasive action.

IV. CONCLUSION AND FUTURE WORK

The capability of sensing contact on the whole body of a robot is an important step for enabling safe and more advanced, intuitive human-robot interactions. In this paper a design of a flexible, stretchable skin that can detect location within a typical 5.7mm resolution was presented. The construction exploited superior CNT-PDMS properties, conductive fabric and a 2D potentiometer concept for position and demonstrated that the same system can also provide a crude estimate of contact force. The application of this smart skin sensor has also been demonstrated in both an automatic emergency stop system as well as a sensor for interactive robotic environments.

Repeatedly stretching this sensor does not influence its localization error significantly. Localization accuracy is potentiometric and will not be effected by stretching but additional study is required to quantify this. By design, the skin's durability is determined primarily by the PDMS substrate. PDMS is among the most durable stretchable elastomers available for typical manufacturing implying that the skin sensor exhibits favorable durability. The minimum threshold force and sensitivity are tunable via mesh size, elastomer, and fabric mechanical properties. Multiple force thresholds are possible via multiple layers.

The application of this design is not limited only to robotics and machinery, but can also be applied to medical

devices, specifically prosthetics. Prosthetics are very similar to robotics as they are a robotic extension of an appendage without the human sense of touch [3]. With this design, localized feedback to the operator may be possible as per neural interface methods in [13] but at a substantially lower cost and manufacturing complexity than their sensor design.

Future work will include more comprehensive quantitative analysis of positional and force accuracy over the entire surface, different sensor sizes, different biaxial strain conditions, conformance to a wider range of robotic link geometries, and contact detection for a wider variety of objects. Different sensing modalities will also be tested such as current difference methods which will require a constant current source or current sensing. The force estimation model will also be improved upon when the manufacturing tolerances for the PDMS-CNT surface are improved.

ACKNOWLEDGMENT

The authors would like to thank Wade Eichhorn and 7-SIGMA Inc. (Minneapolis, MN) for donating their PDMS-CNT conformable sensor technology and related supplies.

REFERENCES

- [1] S. Haddadin, A. Albu-Schäffer, and G. Hirzinger, "Requirements for safe robots: Measurements, analysis and new insights," *The International Journal of Robotics Research*, vol. 28, no. 11-12, pp. 1507–1527, 2009.
- [2] R. S. Dahiya, G. Metta, M. Valle, and G. Sandini, "Tactile sensing from humans to humanoids," *Robotics, IEEE Transactions on*, vol. 26, no. 1, pp. 1–20, 2010.
- [3] J.-H. Kim, J.-I. Lee, H.-J. Lee, Y.-K. Park, M.-S. Kim, and D.-I. Kang, "Design of flexible tactile sensor based on three-component force and its fabrication," in *IEEE International Conference on Robotics and Automation*, 2005.
- [4] J. H. Shan, T. Mei, L. Sun, D. Y. Kong, Z. Y. Zhang, L. Ni, M. Meng, and J. R. Chu, "The design and fabrication of a flexible three-dimensional force sensor skin," in *IEEE International Conference on Intelligent Robots and Systems*, 2005.
- [5] J. Ulmen and M. Cutkosky, "A robust, low-cost and low-noise artificial skin for human-friendly robots," in *IEEE International Conference on Robotics and Automation*, 2010.
- [6] Y. R. Wang, J. M. Zheng, G. Y. Ren, P. H. Zhang, and C. Xu, "A flexible piezoelectric force sensor based on pvdff fabrics," *IOP Smart Materials and Structures*, vol. 20, pp. 1–7, 2011.
- [7] B. Choi, H. R. Choi, and S. Kang, "Development of tactile sensor for detecting contact force and slip," in *IEEE Intelligent Robots and Systems*, 2005.
- [8] T. V. Papakostas, J. Lima, and M. Lowe, "A large area force sensor for smart skin applications," in *Proceedings of IEEE Sensors*, 2002.
- [9] G. Pugach, V. Khomenko, A. Melnyk, A. Pitti, P. Henaff, and P. Gaussier, "Electronic hardware design of a low cost tactile sensor device for physical human-robot interactions," in *IEEE International Scientific Conference Electronics and Nanotechnology*, 2013.
- [10] M.-A. Lacasse, V. Duchaine, and C. Gosselin, "Characterization of the electrical resistance of carbon-black-filled silicone: Application to a flexible and stretchable robot skin," in *IEEE International Conference on Robotics and Automation*, 2010.
- [11] R. Walz, Z. Meier, M. Winek, and T. M. Kowalewski, "Medical simulators for developing countries via low-cost two-dimensional position tracking," *ASME Journal of Medical Devices*, vol. 8, pp. 1–3, 2014.
- [12] J. J. O'Neill and T. M. Kowalewski, "Online free anatomy registration via non-contact skeletal tracking for collaborative human/robot interaction in surgical robotics," *ASME Journal of Medical Devices*, 2014.
- [13] J. Kim, M. Lee, H. J. Shim, R. Ghaffari, H. R. Cho, D. Son, Y. H. Jung, M. Soh, C. Choi, S. Jung, *et al.*, "Stretchable silicon nanoribbon electronics for skin prosthesis," *Nature communications*, vol. 5, 2014.